Spectroscopic studies of Eu^{3+} and Dy^{3+} centers in ThO_2

M. Yin*
Groupe de Radiochimie, Institut de Physique Nucleaire, Boîte Postale 1, 91406 Orsay Cedex, France and Department of Physics, University of Science and Technology of China, 230026 Hefei, China

J-C. Krupa
Groupe de Radiochimie, Institute de Physique Nucleaire, Boîte Postale 1, 91406 Orsay Cedex, France

E. Antic-Fidancev
Laboratoire de Chimie Appliquée de l'Etat Solide-Centre National de la Recherche Scientifique-Unit Mixte de Recherche 7574, Ecole Nationale Supérieure de Chimie de Paris, 11, Rue Pierre et Marie Curie, 75231 Paris Cedex 05, France

A. Lorriaux-Rubbens
Laboratoire de Spectroscopie Infrarouge et Raman, Universite des Sciences et Technologies de Lille, 59655 Villeneuve d'Ascq Cedex, France
(Received 7 October 1999)

Luminescence and excitation spectra of $\mathcal{R}^{3+}$-doped thorium oxide ($\mathcal{R}^{3+}=Eu^{3+}, Dy^{3+}$) are reported and analyzed. ThO_2 was synthesized and grown as crystal using the flux technique. Usually, $\mathcal{R}^{3+}$ ions substitute Th^{4+} as a cubic site, but charge compensation often results in the presence of other centers. Doping concentration also has an important effect on the formation of the crystallographic sites. Using selective dye laser excitation at 12 K and selection rules, site symmetries of Eu^{3+} and Dy^{3+} ions in ThO_2 are determined and fluorescence from different centers is isolated. Results show that under conditions investigated, Eu^{3+} ions have O_h and C_{3v} site symmetry in ThO_2 while for Dy^{3+} only C_{3v} exists. Lifetimes were measured and discussed. A crystal-field (cf) calculation has been performed on the reduced ^7F_J basis of the ground ^7F term of the Eu^{3+} ion. The crystal-field parameter set is then used to calculate Dy^{3+} energy levels in ThO_2 as a test of its consistency.

I. INTRODUCTION

Thorium dioxide is an interesting host matrix for a variety of reasons. It crystallizes in the fluorite structure with a lattice constant of 0.56 nm. The ionic radius of Th^{4+} is 0.104 nm, making the substitution of all of the rare earths possible. The luminescence of Eu^{3+} in thorium dioxide has been studied by several authors. Breysse and Faure[1] and Hubert and co-workers[2,3] studied powder samples. The former authors concentrated on the influence of preparation condition on luminescence properties, while the latter ones focused on the comparison with Am^{3+} ions. Linares,[4] in 1966, studied single crystals at low concentration of the activator (0.5%) and x-ray excitation. In all cases, the emission was described as contributions from several sites of different symmetry (cubic and noncubic), but no one gave a detailed study for different sites by using selective excitation at low temperature. In the case of ThO_2:Dy, to our best knowledge, no literature on spectroscopic results can be found.

In this paper we give a detailed study on the spectroscopic properties of Eu^{3+}- and Dy^{3+}-doped ThO_2 (luminescence spectra, excitation spectra, lifetimes, cross relaxation). The contributions from the cubic symmetry (O_h) and trigonal symmetry (C_{3v}) of Eu^{3+} ion sites in ThO_2 are distinguished by using selective excitation at low temperature. Energy levels and lifetimes of Eu^{3+} and Dy^{3+} ions in the different sites are tabulated and discussed. Semiempirical calculations were performed on the Eu^{3+} ion and the obtained crystal-field parameters were used to reproduce the energy-level diagram of Dy^{3+} in ThO_2 as a test of their validity.

II. EXPERIMENT

The crystals were grown by the flux method and display light yellow (ThO_2:Eu^{3+}) and blue (ThO_2:Dy^{3+}) color, respectively. For luminescence studies, we used a YAG:Nd^{3+} (where YAG is yttrium aluminum garnet) laser (20W Quantel), a dye laser (coumarin 480, coumarin 500, and rhodamine 610), and a Jobin-Yvon HR-1000 monochromator with a dispersion of 0.8 nm/mm. The samples were placed in a liquid-helium optical cryostat (OXFORD International) with a regulated heated gas system allowing the temperature to be varied between 10–300 K. The photons were detected by a Hamamatsu R374 photomultiplier and the output signals were fed into a Standford SR510 lock-in amplifier. A Lecroy 9350M oscilloscope (500 MHz) interfaced with a computer was used for transient measurements.

III. RESULTS AND DISCUSSION

In ThO_2, Th^{4+} ions occupy a site of O_h symmetry. Replacing tetravalent ions by trivalent ions will require positive charge compensation to maintain the electrical neutrality. The compensation can be achieved at some distance by Th^{4+} interstitial ions. Then several centers are expected in this matrix. Apparently, the doping concentration has a very important role in determining the site symmetry.[4,5] Linares[4] studied the problem and came to the conclusion that the cubic sites O_h would be predominated at low rare-earth concentration and the trigonal C_{3v} at high concentration.

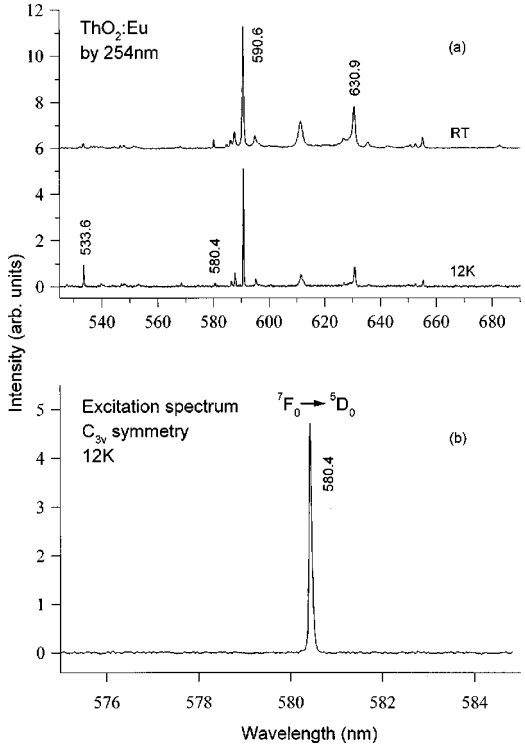

FIG. 1. (a) Emission spectra of ThO_2:Eu under 254-nm excitation at 12 K and RT; (b) excitation spectrum of ThO_2:Eu at 12 K. Luminescence detected at 630.9 nm.

A. ThO_2:Eu^{3+}

1. Determination of O_h and C_{3v} symmetry

In a first step, a global view of the emission spectra is obtained by excitation in the Eu-O charge-transfer band at 254 nm from a mercury lamp [Fig. 1(a)]. The magnetic dipole (MD) transition $^5D_0 \rightarrow {}^7F_1$ at 590.6 nm (16 932 cm^{-1}) is the main emission line observed at room and low temperature, showing again the typical behavior of Eu^{3+} ions in such a cubic matrix with an inversion center in the symmetry

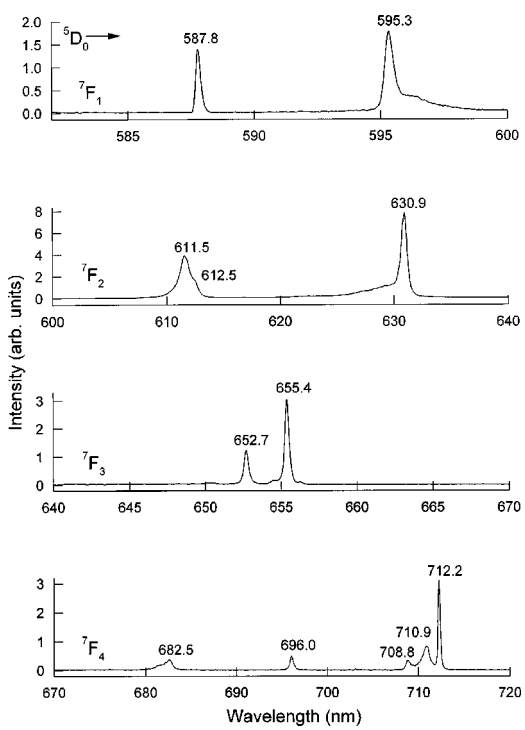

FIG. 2. Emission spectra of ThO_2:Eu at 12 K under excitation at 580.4 nm, see Fig. 1.

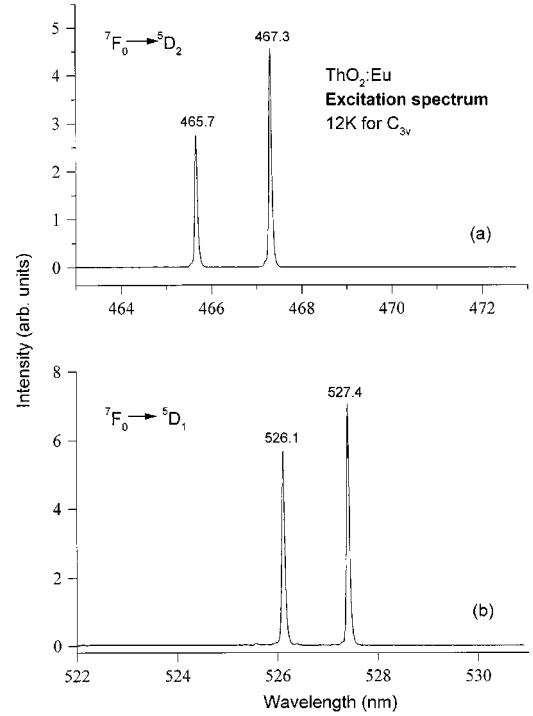

FIG. 3. Excitation spectra for 630.9-nm emission ($^5D_0 \rightarrow {}^7F_2$) of Eu^{3+} ions in C_{3v} site in ThO_2. (a) $^7F_0 \rightarrow {}^5D_2$ transition region, (b) $^7F_0 \rightarrow {}^5D_1$ transition region.

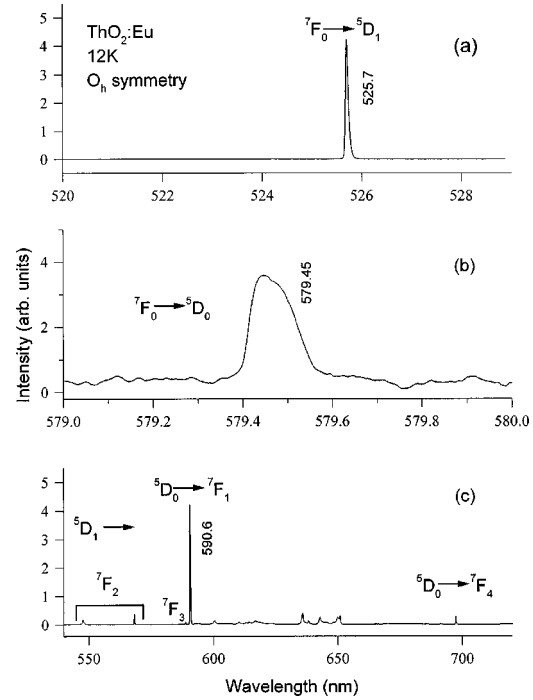

FIG. 4. (a) Excitation spectra for 590.6-nm emission ($^5D_0 \rightarrow {}^7F_1$) of O_h site of ThO_2:Eu in the $^7F_0 \rightarrow {}^5D_1$ transition region, (b) $^7F_0 \rightarrow {}^5D_0$ transition region. (c) Emission spectrum of the O_h site of ThO_2:Eu at 12 K using $^5D_1$ excitation at 525.7 nm.

TABLE I. Transition energies of Eu^{3+} ions in ThO_2 obtained from excitation and emission spectra at 12 K. Energy levels are given at the right column.

Transitions	Observed lines: Wavelength (nm)	Observed lines: Wave number (cm^{-1})	Experimental: Energy levels (cm^{-1})	Experimental: $^{2S+1}L_J$ level
	(a) C_{3v} site			
$^7F_0 \rightarrow {}^5D_2$	465.7	21 473	21 473	$^5D_2$
	467.3	21 400	21 400	
$^7F_0 \rightarrow {}^5D_1$	526.1	19 008	19 008	$^5D_1$
	527.4	18 961	18 961	
$^5D_1 \rightarrow {}^7F_1$	533.5	18 742	219	$^7F_1$
	539.6	18 532	429	
$^5D_1 \rightarrow {}^7F_2$	552.9	18 086	875	$^7F_2$
	568.7	17 584	1377	$^7F_2$
$^7F_0 \rightarrow {}^5D_0$	580.4	17 229	0 ($^7F_0$)	17 229 ($^5D_0$)
$^5D_1 \rightarrow {}^7F_3$	584.6	17 106	1855	$^7F_3$
	586.4	17 053	1908	
	587.8	17 013	1948	
	589.2	16 972	1989	
$^5D_0 \rightarrow {}^7F_1$	587.8	17 013	216	$^7F_1$
	595.3	16 798	431	
$^5D_0 \rightarrow {}^7F_2$	611.5	16 353	876	$^7F_2$
	612.5	16 327	902	
$^5D_1 \rightarrow {}^7F_4$	621.2	16 098	2863	$^7F_4$
	626.9	15 952	3009	
$^5D_0 \rightarrow {}^7F_2$	630.9	15 850	1379	$^7F_2$
$^5D_0 \rightarrow {}^7F_3$	650.4	15 375	1854	$^7F_3$
	652.7	15 321	1908	
	654.5	15 279	1950	
	655.4	15 258	1971	
	656.2	15 239	1990	
$^5D_0 \rightarrow {}^7F_4$	682.5	14 652	2577	$^7F_4$
	696.0	14 368	2861	
	708.8	14 108	3121	
	710.9	14 067	3162	
	712.2	14 041	3188	
$^5D_1(1) \rightarrow {}^7F_5$	668.3	14 963	3998	$^7F_5$
	669.7	14 932	4029	
	(b) O_h site			
$^7F_0 \rightarrow {}^5D_2$	467.0	21 415	21 415	$^5D_2$
$^7F_0 \rightarrow {}^5D_1$	525.7	19 022	19 022	$^5D_1$
$^5D_2 \rightarrow {}^7F_3$	512.4	19 516	1899	$^7F_3$
	516.0	19 380	2035	
$^5D_1 \rightarrow {}^7F_2$	547.67	18 259	763	$^7F_2$
	568.17	17 600	1422	
$^7F_0 \rightarrow {}^5D_0$	579.45	17 258	0 ($^7F_0$)	17 258 ($^5D_0$)
$^5D_1 \rightarrow {}^7F_3$	588.67	16 987	2035	$^7F_3$
$^5D_0 \rightarrow {}^7F_1$	590.6	16 932	326	$^7F_1$
$^5D_0 \rightarrow {}^7F_4$	697.34	14 340	2918	$^7F_4$

elements. But the appearance of several weaker lines in the spectra in addition to the allowed transitions for O_h symmetry indicates that other Eu^{3+} sites may be coexisting. Among the weaker emission lines in Fig. 1(a), the 630.9 nm (15 850 cm^{-1}) is the strongest one. Excitation spectrum [Fig. 1(b)] obtained by monitoring at this line gives a sharp absorption peak at 580.4 nm, corresponding to the $^7F_0 \rightarrow {}^5D_0$ transition of Eu^{3+} in the site under investigation. In Fig. 2, the emission spectra of ThO_2:Eu^{3+} in this particular site, obtained under 580.4 nm selective excitation at 12 K, are plotted and the transitions assigned. From comparison between Figs. 2 and 1(a) (12 K) the conclusion come out that all the peaks in the range of 600.0–670.0 nm (corresponding to $^5D_0 \rightarrow {}^7F_{2,3}$ transitions) in Fig. 1(a) belong to the same site. It suggests that there are only two sites in ThO_2:Eu^{3+}, including O_h.

TABLE II. Lifetimes of ^5D_J levels of Eu^{3+} ions in O_h and C_{3v} sites in the ThO_2 matrix at room temperature (RT) and 12 K.

Level	Lifetime (ms): RT	Lifetime (ms): 12 K
	(a) C_{3v} site	
$^5D_0$	0.84	0.86
$^5D_1$	0.11	0.17
$^5D_2$	0.18	0.25
	(b) O_h site	
$^5D_0$	3.73	5.27
$^5D_1$	0.15	0.25

Here again, the Eu^{3+} ion is used as a local crystal-field probe to characterize the site symmetry, as done by different authors previously, e.g., Refs. 6 and 7. Figure 2 tells us that there are two, three, and five peaks which can be attributed respectively to $^5D_0 \rightarrow {}^7F_1$, $^5D_0 \rightarrow {}^7F_2$, and $^5D_0 \rightarrow {}^7F_4$ transitions. According to the selection rules, two peaks for $^5D_0 \rightarrow {}^7F_1$ transitions is an indication that the point group could be hexagonal, trigonal, or tetragonal. Then, three peaks for $^5D_0 \rightarrow {}^7F_2$ transitions further indicates that the symmetry could be S_4, C_{3v}, or C_3, and at last from the five peaks recorded for $^5D_0 \rightarrow {}^7F_4$ transitions we come to the conclusion that the site symmetry is C_{3v}, consistent with our analysis at the beginning of this section.

It should be pointed out that in the above discussion, the assumption that the $^5D_0 \rightarrow {}^7F_{2,4}$ transitions are pure electrical dipole (ED) transitions and $^5D_0 \rightarrow {}^7F_1$ pure MD is used. This is widely accepted and being used in publications.[8,9]

2. Energy levels

From Figs. 1 and 2, the energy of $^5D_0$ and all the $^7F_{0-4}$ crystal-field levels of Eu^{3+} ions in C_{3v} symmetry were measured (there are five peaks for $^5D_0 \rightarrow {}^7F_3$ transitions, but we only marked the two strongest ones for clarity). The excitation spectrum of λ_{em}=630.9-nm emission line in the range of 522–530 nm [Fig. 3(b)] confirmed two peaks for $^7F_0 \rightarrow {}^5D_1$ transitions in C_{3v} measured at 19 008 cm^{-1} (526.1 nm) and 18 961 cm^{-1} (527.4 nm) and the excitation spectrum in the range 463–473 nm [Fig. 3(a)] gives us the energy of two crystal-field levels of the $^5D_2$ multiplet. According to the selection rules, there should be three peaks for the $^7F_0 \rightarrow {}^5D_2$ transition, but the third one may be too weak to be recorded. Selective excitation in these ^5D_J (J=1,2) C_{3v} levels at low temperature provides some other peaks and

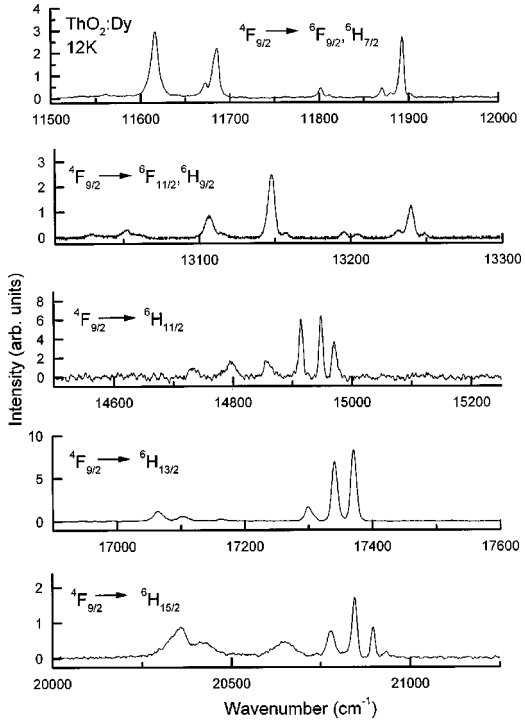

FIG. 5. Emission spectra of ThO_2:Dy under 254-nm excitation at 12 K.

consequently more energy levels can be assigned. Table I(a) is a summary of the obtained 22 energy levels of Eu^{3+} ions in C_{3v} symmetry in ThO_2.

As stated before, for Eu^{3+} ions in O_h symmetry offered by the ThO_2 lattice, there is only one strong emission peak at 590.6 nm attributed to $^5D_0 \rightarrow {}^7F_1$ transitions under UV excitation. Then, the key factor to deduce the energy levels of Eu^{3+} ions in O_h symmetry is to determine the position of $^5D_0$ or $^7F_1$ level. In order to get more information, the excitation spectra of 590.6-nm emission were recorded and a $^5D_1$ level at 19 022 cm^{-1} (525.7 nm) [Fig. 4(a)] was first obtained. The excitation spectrum ranging from 579 to 580 nm gave us a very weak and narrow peak at 579.45 nm (17 258 cm^{-1}) [Fig. 4(b)] which was assigned to $^7F_0 \rightarrow {}^5D_0$ electronic transition. While pure electronic transitions are forbidden in O_h symmetry, this line cannot be attributed to a vibronic transition because we know from Raman spectrum that there is only one kind of phonon with energy 465 cm^{-1} and if this peak is assigned as a vibronic line, then the pure 0-0 transition will be located at 16 793 cm^{-1}, far from all the observed $^7F_0 \rightarrow {}^5D_0$ transitions in the full europium nephelauxetic scale.[10] The existence of a pure $^7F_0 \rightarrow {}^5D_0$ transition may be due to a small distortion in the cubic site, which can be related to the radius difference between the embedded ion Eu^{3+}(0.095 nm) and the substituted ion Th^{4+} (0.104 nm). Similar phenomena were also observed in other cubic symmetry.[5]

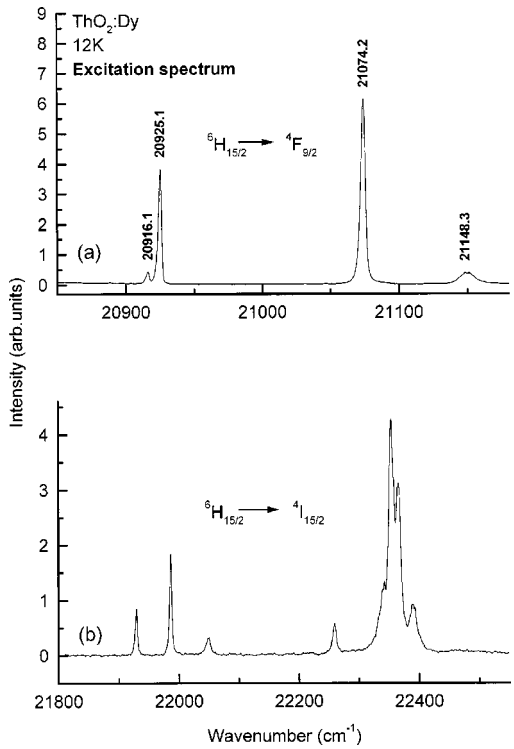

FIG. 6. Excitation spectrum for $^4F_{9/2} \rightarrow {}^6H_{13/2}$ emission from Dy^{3+} ions in ThO_2 at 12 K.

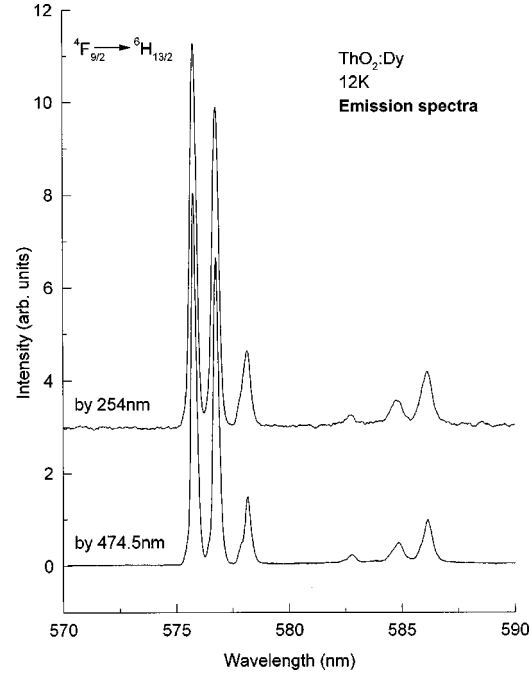

FIG. 7. Emission spectra of ThO_2:Dy in the region of 570–590 nm at 12 K using 254 and 474.5 nm (21 074.2 cm^{-1}) excitation, respectively, see Fig. 6.

Similarly to C_{3v} symmetry, site selective excitation [Fig. 4(c)] gave information about energy levels of Eu^{3+} in O_h symmetry and Table I(b) summarized the obtained nine level energies.

3. Lifetime measurement and energy transfer

As seen before, Eu^{3+} ions in ThO_2 occupy O_h and C_{3v} sites. One can expect that substitution into the O_h site will give a longer lifetime than substitution into the C_{3v} site of lower symmetry. Table II shows lifetimes of the ^5D manifold for C_{3v} and O_h symmetries at both 12 K and room temperature. All the values were obtained by exciting the level directly except for the $^5D_0$ level of Eu^{3+} in O_h sym-

TABLE III. Transition energies of Dy^{3+} ions in ThO_2 obtained from excitation and emission spectra at 12 K.

Transitions	Observed lines (cm^{-1})	Experimental Energy levels (cm^{-1})	$^{2S+1}L_J$ level
$^6H_{15/2} \rightarrow {}^4F_{9/2}$	20 916	20 916	$^4F_{9/2}$
	20 925	20 925	
	21 074	21 074	
	21 148	21 148	
$^6H_{15/2} \rightarrow {}^4I_{15/2}$	21 929	21 929	$^4I_{15/2}$
	21 986	21 986	
	22 050	22 050	
	22 259	22 259	
	22 342	22 342	
	22 354	22 354	
	22 366	22 366	
	22 388	22 388	
$^4F_{9/2} \rightarrow {}^6H_{15/2}$	20 933	0	$^6H_{15/2}$
	20 897	36	
	20 845	88	
	20 780	153	
	20 649	284	
	20 410	523	
	20 359	574	
$^4F_{9/2} \rightarrow {}^6H_{13/2}$	17 371	3562	$^6H_{13/2}$
	17 341	3592	
	17 299	3634	
	17 162	3771	
	17 103	3830	
	17 064	3869	
$^4F_{9/2} \rightarrow {}^6H_{11/2}$	14 970	5963	$^6H_{11/2}$
	14 948	5985	
	14 914	6019	
	14 855	6078	
	14 796	6137	
	14 732	6201	
$^4F_{9/2} \rightarrow {}^6F_{11/2} + {}^6H_{9/2}$	13 249	7684	$^6F_{11/2} + {}^6H_{9/2}$
	13 240	7693	
	13 232	7701	
	13 205	7728	
	13 196	7737	
	13 157	7776	
	13 148	7785	
	13 106	7827	
	13 052	7881	
	13 028	7905	
	12 949	7984	
$^4F_{9/2} \rightarrow {}^6F_{9/2} + {}^6H_{7/2}$	11 902	9031	$^6F_{9/2} + {}^6H_{7/2}$
	11 893	9040	
	11 880	9053	
	11 871	9062	
	11 812	9121	
	11 802	9131	
	11 686	9247	
	11 673	9260	
	11 616	9317	
	11 561	9372	

TABLE IV. Experimental and calculated energy-level schemes for Eu^{3+} in ThO_2 for the C_{3v} site.

$^{2S+1}L_J$ level	E expt. (cm^{-1})	E calc. (cm^{-1})	Irreducible representation
$^7F_0$	0	0	A_1
$^7F_1$	216	218	A_2
	431	430	E
$^7F_2$	876	892	A_1
	902	900	E
	1379	1373	E
$^7F_3$	1854	1857	E
	1908	1911	A_1
	1950	1943	A_2
	1971	1970	E
	(1990)	2138	A_2
$^7F_4$	2577	2572	A_1
	2861	2848	E
	3009	3001	A_2
	3121	3126	E
	3162	3172	A_1
	3188	3198	E

TABLE V. Crystal-field parameters for Eu^{3+} in ThO_2 for C_{3v} site symmetry.

Parameter	Value (cm^{-1})
B_0^2	−661
B_0^4	843
B_3^4	−1709
B_0^6	799
B_3^6	299
B_6^6	1028
n levels	16
residue	868
σ	9.3

TABLE VI. Experimental and calculated energy-level schemes for Eu^{3+} in ThO_2 for the O_h site.

$^{2S+1}L_J$ level	E expt. (cm^{-1})	E calc. (cm^{-1})	Irreducible representation
$^7F_0$	0	0	A_1
$^7F_1$	326	326	T
$^7F_2$	763	763	T
	1422	1422	E
$^7F_3$		1858	T
	2035	2035	T
		2251	A_2
$^7F_4$		2290	A_1
	2918	2918	T
		3147	T
	3290	3290	E

TABLE VII. Crystal-field parameters for Eu^{3+} in ThO_2 for O_h site symmetry.

Parameter	Value (cm^{-1})
B_0^2	0
B_0^4	−2247
B_4^4	−1342
B_0^6	1079
B_4^6	−2022
n levels	7
residue	0.7
σ	0.3

metry, where the nearest level of the D_1 multiplet was excited. The lifetime enhancement for O_h symmetry was approximately six times over the C_{3v} one and the largest difference is for the $^5D_0$ level at low temperature. The table also shows that $^5D_1$ and $^5D_2$ levels have as expected a shorter lifetime than $^5D_0$ accordingly to the energy gaps between close levels. It is interesting to notice that for the $^5D_1$ (C_{3v}) emitting level, the decay time decreases rapidly as the temperature increases, from 0.17 ms at 12 K to 0.11 ms at 300 K, while for $^5D_0$ (C_{3v}) the lifetime nearly remains constant for different temperatures. This is due to an enhanced energy transfer from $^5D_1$ to $^5D_0$ at higher temperatures.[11] Indeed, Fig. 1(a) (normalized for the 590.6-nm line) clearly shows the phenomena. The sequence of the relative intensity of 533.6- and 580.4-nm emission lines, which correspond to the $^5D_1 \rightarrow {}^7F_1$ and $^5D_0 \rightarrow {}^7F_0$ transition of Eu^{3+} ions in C_{3v} sites, respectively, is varying from 300 to 12 K. The enhanced energy transfer

$$^5D_1 + {}^7F_0 \rightarrow {}^5D_0 + {}^7F_3$$

at room temperature results in the quenching of the $^5D_1$ level emission in favor of the lower $^5D_0$ energy-level emission, and consequently contributes to a shorter lifetime for the $^5D_1$ emitting level when the temperature increases.

B. ThO_2:Dy^{3+}

Differently from Eu^{3+}, Dy^{3+} in ThO_2 has only one emitting level of $^4F_{9/2}$ in the visible range.[12] Figure 5 is the emission spectra of ThO_2:Dy^{3+} in the region of 11 500–21 250 cm^{-1} under 254-nm excitation at 12 K. The spectra consist of five line groups, corresponding to $^4F_{9/2} \rightarrow {}^6F_{9/2} + {}^6H_{7/2}$, $^4F_{9/2} \rightarrow {}^6F_{11/2} + {}^6H_{9/2}$, $^4F_{9/2} \rightarrow {}^6H_{11/2}$, $^4F_{9/2} \rightarrow {}^6H_{13/2}$, and $^4F_{9/2} \rightarrow {}^6H_{15/2}$ transitions, respectively. Following the spectroscopic studies of Eu^{3+} ions in ThO_2, there are two sites of O_h and C_{3v} symmetry available for the trivalent rare-earth ions. In order to know the symmetry properties of the crystal field acting on Dy^{3+} ions in the matrix, the excitation spectrum of $^4F_{9/2} \rightarrow {}^6H_{13/2}$ emissions for Dy^{3+} ions in ThO_2 was measured (Fig. 6). The strongest excitation is located at 21 074.2 cm^{-1} (474.5 nm). Selective excitation at 474.5 nm gives exactly the same emission spectrum as nonselective excitation at 254 nm (Fig. 7). This result suggests that there is only one site for Dy^{3+} ions in ThO_2.

We are thinking that the site symmetry is C_{3v} rather than O_h. Indeed, Fig. 6(b) shows that $^4I_{15/2}$ has eight crystal-field

TABLE VIII. Experimental and calculated energy-level schemes for Dy^{3+} in ThO_2. Free ion parameters from Table IX and CFP's from Table V.

$^{2S+1}L_J$ level	E expt. (cm^{-1})	E calc (cm^{-1})
$^6H_{15/2}$	0	−2
	26	40
	88	107
	153	218
	284	347
	523	551
	574	600
		624
$^6H_{13/2}$	3562	3585
	3592	3600
	3634	3618
	3772	3771
	3830	3855
	3869	3864
		3907
$^6H_{11/2}$	5963	5968
	5985	5977
	6019	5983
	6078	6079
	6138	6111
	6201	6185
$^6H_{9/2}+{}^6F_{11/2}$	7684	7625
	7693–7701	7688
	7728–7737	7711
	7776–7785	7804
	7827	7856
	7881	7912
	7905	7928
	7984	8020
		8056
		8210
		8276
$^6H_{7/2}+{}^6F_{9/2}$	9031–9040	9023
	9053–9062	9060
	9121–9131	9111
	9247	9306
	9260	9328
	9317	9354
	9732	9412
		9463
		9680
$^4F_{9/2}$	20 916–20 925	20 927
	21 074	21 019
	21 148	21 086
		21 208
		21 567
$^4I_{15/2}$	21 929	21 899
	21 986	21 959
	22 050	22 018
	22 259	22 250
	22 342	22 335
	22 354	22 395
	22 366	22 415
	22 388	22 443

TABLE IX. Free ion parameters for Dy^{3+} in ThO_2: values taken from Ref. 18.

Parameter	Value (cm^{-1})
E^0	55 395
E^1	6158.06
E^2	30.43
E^3	622.75
α	17.92
β	−612.15
γ	1679.85
T^2	339.14
T^3	74.13
T^4	49.74
T^6	−316.25
T^7	366.15
T^8	362.65
ς	1914

sublevels. This ruled out the possibility of O_h symmetry for which the maximum splitting multiplicity of $^4I_{15/2}$ is 6. According to the results obtained for ThO_2:Eu^{3+}, it is reasonable to attribute the site symmetry as C_{3v}. Experimental results supported the argument. For example, the selection rules and the splitting number of the $^6H_{13/2}$ level in C_{3v} symmetry agrees well with the seven peaks observed for the transitions of $^4F_{9/2}\rightarrow{}^6H_{13/2}$ (Fig. 7). The only C_{3v} symmetry observed for Dy^{3+} in ThO_2 results from the higher doping concentration. Table III summarized the experimental transition lines at 12 K and the deduced energy levels of Dy^{3+} in ThO_2.

The lifetime of the $^4F_{9/2}$ level of Dy^{3+} in ThO_2 (0.40 ms) does not change with temperature. The phenomenon can be explained by the large energy gap (about 6000 cm^{-1}) between the $^4F_{9/2}$ and $^6F_{1/2}$ levels as well as by nonefficient cross relaxation occurring among levels.

C. Crystal field

The usual way to fit the energy levels of a given rare-earth ion embedded in a crystalline medium is to treat different interactions simultaneously. The basis of these procedures is given by Judd[13] and Wybourne,[14] respectively. In this work we consider only the crystal-field contribution which is expressed as a sum of tensorial operators:

$$H_{cf}=\sum_{k,q,i} B_q^k(C_q^k).$$

B_q^k are the phenomenological crystal-field parameters (CFP) and their number depends on the local point site symmetry of the rare-earth ion. The potential for the C_{3v} site symmetry is described by six nonzero coefficients, B_q^k CFP's, and nine C_q^k operators,[16,17]

$$H_{C_{3v}}=B_0^2(C_0^2)+B_0^4(C_0^4)+B_3^4(C_{-3}^4-C_3^4)+B_0^6(C_0^6)+B_3^6(C_{-3}^6+C_3^6)+B_6^6(C_{-6}^6+C_6^6).$$

In the case of the O_h site symmetry, considering the fourfold axis, five nonzero coefficients, B_q^k CFP's, and six C_q^k tensorial operators exist,

$$H_{C_{4v}}=B_0^2(C_0^2)+B_0^4(C_0^4)+B_4^4(C_{-4}^4+C_4^4)+B_0^6(C_0^6)+B_4^6(C_{-4}^6+C_4^6)$$

with $B_0^4/B_4^4=\sqrt{14}/\sqrt{5}$ and $B_0^6/B_4^6=-\sqrt{2}/\sqrt{7}$ with respect to the cubic ratio.

The crystal-field analysis is performed for the Eu^{3+} ion embedded in ThO_2 and the set of the CFP's obtained is then used to simulate the Dy^{3+} ion behavior. The total degeneracy of the $4f^6$ configuration (Eu^{3+} ion) is high, 3003, and the calculation of the CFP's can be done on the strongly reduced ^7F_J basis of the ground ^7F term. For more details see Ref. 15.

Experimental and calculated energy-level schemes for the Eu^{3+} ion in the two different sites C_{3v} and O_h are given in Tables IV and VI and the phenomenological crystal-field parameters are listed in Tables V and VII. It should be mentioned that the level located at the 1990 cm^{-1}, C_{3v} site, was not used in the fit. This line, appearing as very weak in the emission spectrum, is suspicious because from the $^7F_3$ multiplet barycenter position, the highest $^7F_3$ component is calculated to be located at about 2140 cm^{-1}.

The CFP set from Table V is used to calculate the Dy^{3+} ion in the ThO_2 matrix as a test of its reliability. The free ion parameters are from DyOF data.[18] The fit which is obtained without trying to adjust the parameter values is quite good, giving some consistency to the parameter set (see Tables VIII and IX).

IV. CONCLUSION

We have carried out a detailed luminescence study of Eu^{3+} and Dy^{3+} in ThO_2. All the assignments are based on the selective excitation and emission spectra at low temperature. Eu^{3+} occupies the cubic (O_h) and trigonal (C_{3v}) sites in ThO_2. The former predominates at low concentration, while the more heavily doped Dy^{3+} only C_{3v} site has been detected. The energy levels and lifetimes of Eu^{3+} and Dy^{3+} ions in different sites are tabulated and discussed.

ACKNOWLEDGMENT

This work was partly supported by the National Natural Science Foundation of China (No. 19774052).

*Electronic address: yinmin@ustc.edu.cn

[1] M. Breysse and L. Faure, J. Lumin. **26**, 107 (1981).
[2] S. Hubert and P. Thouvenot, J. Alloys Compd. **180**, 193 (1992).
[3] S. Hubert, P. Thouvenot, and N. Edelstein, Phys. Rev. B **48**, 5751 (1993).
[4] R. C. Linares, J. Opt. Soc. Am. **56**, 1700 (1966).
[5] J. P. Jouart, C. Bissieux, M. Egee, G. Mary, and M. de Murcia, J. Phys. C **14**, 4923 (1981).
[6] S. P. Sinha and E. Butter, Mol. Phys. **16**, 285 (1969).
[7] N. Mercier, E. Antic-Fidancev, M. Lemaitre-Blaise, and M. Leblanc, J. Solid State Chem. **132**, 33 (1997).
[8] G. Blasse and A. Bril, J. Chem. Phys. **45**, 3327 (1966).

[9] C. Gorller-Walrand and K. Binnemans, *Rationalization of Crystal-Field Parametrization*, edited by K. A. Gschneidner, Jr. and L. Eyring in Handbook on the Physics and Chemistry of Rare Earths Vol. 23 (Elsevier, Amsterdam, 1996).

[10] E. Antic-Fidancev, J. Alloys Compds. (to be published).

[11] G. Blasse and B. C. Grabmaier, *Luminescent Materials* (Springer-Verlag, Berlin, 1994).

[12] D. R. Foster and F. S. Richardson, J. Chem. Phys. **82**, 1085 (1985).

[13] B. R. Judd, Phys. Rev. **141**, 4 (1966).

[14] B. G. Wybourne, *Spectroscopic Properties of Rare Earths* (Interscience, New York, 1965).

[15] G. Corbel, M. Leblanc, E. Antic-Fidancev, and M. Lemaitre-Blaise, J. Solid State Chem. **144**, 35 (1999).

[16] J. L. Prather, *Atomic Energy Levels in Crystals*, Natt. Bur. Stand. (U.S.) Monograph No. 19 (U.S. GPO, Washington, D.C., 1961).

[17] P. Caro, Structure *Electronique des Elements de Transition* (Presses Universitaires de France, Paris, 1976).

[18] J. Holsa, E. Kestila, R. Saez-Puche, P. Deren, W. Strek, and P. Porcher, J. Phys.: Condens. Matter **8**, 1575 (1996).